OXFORD

SOT | Society of Toxicology
www.toxsci.oxfordjournals.org

TOXICOLOGICAL SCIENCES, 154(2), 2016, 403–415

doi: 10.1093/toxsci/kfw174
Advance Access Publication Date: September 9, 2016
Research article

Transient Proteotoxicity of Bacterial Virulence Factor Pyocyanin in Renal Tubular Epithelial Cells Induces ER-Related Vacuolation and Can Be Efficiently Modulated by Iron Chelators

Valeri V. Mossine,[*,†,1] James K. Waters,[†] Deborah L. Chance,[‡,§] and Thomas P. Mawhinney[*,†,§]

[*]Department of Biochemistry, [‡]Department of Molecular Microbiology and Immunology, [§]Department of Child Health, University of Missouri, Columbia, Missouri 65211; and [†]Experiment Station Chemical Labs, University of Missouri, Columbia, Missouri 65211

[1]To whom correspondence should be addressed at Department of Biochemistry, University of Missouri, Agriculture Building, Room 4, Columbia, MO 65211, USA. Fax: (573) 884-4631. E-mail: mossinev@missouri.edu.

ABSTRACT

Persistent infections of biofilm forming bacteria, such as *Pseudomonas aeruginosa*, are common among human populations, due to the bacterial resistance to antibiotics and other adaptation strategies, including release of cytotoxic virulent factors such as pigment pyocyanin (PCN). Urinary tract infections harbor *P. aeruginosa* strains characterized by the highest PCN-producing capacity, yet no information is available on PCN cytotoxicity mechanism in kidney. We report here that renal tubular epithelial cell (RTEC) line NRK-52E responds to PCN treatments with paraptosis-like activity features. Specifically, PCN-treated cells experienced dilation of endoplasmic reticulum (ER) and an extensive development of ER-derived vacuoles after about 8 h. This process was accompanied with hyper-activation of proteotoxic stress-inducible transcription factors Nrf2, ATF6, and HSF-1. The cells could be rescued by withdrawal of PCN from the culture media before the vacuoles burst and cells die of non-programmed necrosis after about 24–30 h. The paraptosis-like activity was abrogated by co-treatment of the cells with metal-chelating antioxidants. A microscopic examination of cells co-treated with PCN and agents aiming at a variety of the cellular stress mediators and pathways have identified iron as a single most significant co-factor of the PCN cytotoxicity in the RTECs. Among biologically relevant metal ions, low micromolar Fe^{2+} specifically mediated anaerobic oxidation of glutathione by PCN, but catechol derivatives and other strong iron complexing agents could inhibit the reaction. Our data suggest that iron chelation could be considered as a supplementary treatment in the PCN-positive infections.

Key words: Pyocyanin; iron; glutathione; proteotoxic stress response; renal tubular epithelial cells; endoplasmic reticulum stress.

Bacterial infections involving opportunistic pathogens, i.e., bacteria targeting critically ill or immunocompromised patients, have recently received alarming reviews due to a rise in their drug resistance associated with healthcare environments (CDC, 2013; Miceli *et al.*, 2011; Weinstein *et al.*, 2013). One common opportunistic pathogen *Pseudomonas aeruginosa* alone is responsible for an estimated 51 000 healthcare-associated infections that occur in the US each year, with about 400 deaths per year attributed to these infections (CDC, 2013). To establish a successful and persistent colonization, *P. aeruginosa* developed a number of strategies, including formation of alginate biofilm, release of antibiotics and iron mobilizing siderophores, quorum

sensing for the population control and so forth (Gellatly and Hancock, 2013; Strateva and Mitov, 2011).

Pyocyanin (PCN) is a blue pigment released by pathogenic *P. aeruginosa* in many environments, including sites of the bacterial infection in humans, such as lung/airway, ear, open wounds, urinary tract, or blood. Pyocyanin is believed to play many roles in establishment of *P. aeruginosa* colonies, including assisting with *P. aeruginosa* respiration, nutrition, and suppression of competitor bacteria (Grahl *et al.*, 2013). Pyocyanin is a phenazine derivative and can readily act as a potent non-enzymatic redox catalyst and accelerate autoxidation of many substrates essential for cellular redox homeostasis, such as NAD(P)H (Schwarzer *et al.*, 2008) and thiols (O'Malley *et al.*, 2004). In its reduced form, pyocyanin can assist with mobilization of iron from transferrin (Cox, 1986). In eukaryotes, PCN can promote intracellular oxidative stress, primarily through generation of superoxide (Rada *et al.*, 2008) and inhibition of catalase (O'Malley *et al.*, 2003), whereas its amphiphilic character and DNA intercalating potential (Das *et al.*, 2015) can make this versatile molecule omnipresent in any type of cellular compartments.

Mammalian cells show a multitude of stress responses in presence of pyocyanin (Rada and Leto, 2009), reportedly due to its interruption with mitochondrial respiration, depletion of ATP and accumulation of reactive oxygen species (ROS). However, the nature and extent of the responses strongly depend on the cell type and normally cannot be generalized. For example, in lung, moderate PCN concentrations caused extensive neutrophils loss through apoptosis (Prince *et al.*, 2008), whereas alveolar epithelial cells survived at much higher PCN concentrations and entered the senescent state instead (Muller, 2006). In bronchial epithelial cells, PCN caused functional hyperactivity, which could be restored by small antioxidants (Rada *et al.*, 2011), whereas the antioxidants were ineffective to counteract loss of functional activity in nasal epithelial cells treated by PCN (Kanthakumar *et al.*, 1994).

Pyelonephritis is a common disease resulting from acute or chronic renal inflammation due to colonization of the kidney tissue by biofilm producing bacteria. Annually, it affects over 300 000 women and over 60 000 men in the US alone (Czaja *et al.*, 2007). Urinary tract infection is the most common source of pyelonephritis, and urine analysis for presence of biofilm-forming bacteria and/or their virulent factors have been long utilized to predict acute pyelonephritis development (Orenstein and Wong, 1999). *P. aeruginosa* pathogen isolated from pyelonephritis sites is characterized by enhanced production of both biofilm and virulence factors (Lagun *et al.*, 2013), which is not surprising, given that PCN is required for biofilm formation by this bacterium (Das *et al.*, 2015). Notably, among all clinical isolates of *P. aeruginosa* obtained from its infection sites, the most potent pyocyanin-producing strains consistently originated from the urinary tract (Al-Ani *et al.*, 1986; Önal *et al.*, 2015; Silva *et al.*, 2014). Despite these facts and high relevance of *P. aeruginosa* virulent factors to morbid kidney infections (Gupta *et al.*, 2013), information on the pyocyanin cytotoxicity in renal cells is lacking.

This account is, to the best of our knowledge, the first report on pyocyanin induced stress in kidney cells. We show a unique pattern of RTECs response to pyocyanin, offer a hypothetical mechanism of its cytotoxicity in RTECs and elucidate a scope of agents able to counteract the cytotoxicity.

MATERIALS AND METHODS

Reagents

Crystalline pyocyanin was purchased from Cayman or prepared by photolysis of 2 mM solution of phenazine methosulfate in 20 mM TRIS buffer, pH 7.4, as reported previously (Cheluvappa, 2014); the crude synthetic pyocyanin was recrystallized from the TRIS buffer and judged essentially pure by its UV–Vis and ESI mass-spectra. Reduced glutathione (GSH) was obtained from Sigma. The GSH and GSSG content in glutathione stock solutions was determined fluorimetrically with *o*-phthaladehyde (Senft *et al.*, 2000). In-house nanopure water was generated by double distillation and used in all experiments. Stock HEPES buffer (200 mM) was treated with 5% (v/v) Chelex resin (BioRad) by stirring overnight. All other commercial reagents, solvents and media were used without any further purification.

Cell Culture

Normal rat kidney tubular epithelial cell line NRK-52E (Heussner and Dietrich, 2013) was purchased from the American Type Culture Collection. The original cells, as well as the NRK-52E based reporter transfects, have been routinely cultured in 1:1 DMEM/F12 Ham (both from Sigma) media mixture supplemented with 5% newborn calf serum (NCS, HyClone) and 1% (v/v) penicillin/streptomycin cocktail (pen/strep, CellGro). This medium is henceforth referred to as the DMEM/F12 complete medium. The cells were subcultured at 1:5 ratio upon reaching near confluency. The standard culturing conditions for all cells were 37 °C, 5% CO_2, and 100% humidity.

Plasmid Constructs

Organelle-targeting reporter vectors *p*mCherry-ER-3 (Plasmid #55041), *p*EGFP-LC3 (Lee *et al.*, 2008) (#24920), *p*mCherry-Lysosomes-20 (#55073), and *p*mCherry-Golgi-7 (#55052) were obtained from Addgene. Super *piggyBac* transposase expression vector was purchased from System Biosciences. Vectors *p*TR01F, *p*TR03F, and *p*TR05F have been previously reported (Mossine *et al.*, 2013).

pTR09F

Two inserts containing 15-bp overhang sequences for the In-Fusion reaction and total of 8 metal response elements for the transcription factor MTF-1 binding (Supplementary Table S1) were synthesized and annealed. The inserts and a product of *p*TR01F (Mossine *et al.*, 2013) digestion with *NheI* and *BglII* were uniformly assembled into *p*TR09F in one step following the In-Fusion reaction according to the manufacturer's (Clontech) protocol.

pTR12F, pTR13F, pTR15F, and pTR31F

Inserts containing 4-bp overhang sequences for the ligation reaction and total of 4, 6, or 8 response elements for each of the transcription factors p53, AP-1, HSF-1, and ATF6, respectively, (Supplementary Table S1) were synthesized and annealed. The inserts and a product of the *p*TR01F digestion with *NheI/BglII* were uniformly assembled into *p*TRnnF in one ligation step. All the constructs were confirmed by DNA sequence analysis.

Transfections

For transient transfections with the organelle-targeting reporter vectors, NRK-52E cells were seeded into wells of a 96-well plate, at 2×10^4 cells per well in the complete DMEM/F12 medium. After 48 h, the adherent cells were treated with the plasmid/Lipofectamine 2000 complexes in Lonza's Renal Epithelial Growth Medium, 200 ng DNA/0.6 μL carrier/100 μL Medium per well. After 24 h, the cells were processed for the treatment schedule, as described in the following section.

For generating stable reporter lines NRK.RnnF, the original NRK-52E cells were seeded into wells of a 96-well plate, at

2×10^4 cells per well in antibiotic-free DMEM/F12 medium supplemented with 5% NCS and left to adhere for 6 h. The cells were then treated with mixtures of 100 ng *p*TRnnF reporter plasmid constructs and 33 ng Super *piggyBac* transposase plasmid complexed with TransIT X2 transfection reagent (Mirus) at 1:2 (μg DNA/μL) ratios. After 16 h, the regular media were added and the cells were left to proliferate for next 48 h. The transfected cells were then treated with the selecting antibiotic (5 μg/mL puromycin) for another week, and the surviving cells were expanded for cryopreservation and activity validation.

Cell Treatment Schedule

Typically, NRK-52E cells or NRK-based reporters were plated in 96-plates (BioLite, Fisher) at 2×10^4 cells/well in 100 μL of the adaptation low-serum medium, which consisted of the DMEM/F12 media mixture supplemented with 2 mg/L insulin, 2 mg/L transferrin, 2 μg/L selenite (2-ITS), 2% NCS, and the pen/strep antibiotic. After 48 h, the adaptation medium was replaced with the Phenol Red-free Corning Serum-free Medium, supplemented with the 2-ITS mixture and the pen/strep (the test medium). Corning Serum-free Medium is a 1:1 mixture of DMEM/F12, containing smaller proportion of RPMI-1640, McCoy's 5A, and 1 g/L BSA. The cells were cultured for next 24 h, after which time, the medium was replaced with fresh test medium containing cytotoxic agents, inhibitors, or carriers for specific times, as indicated.

Cell Proliferation

Cell proliferation was evaluated by either: (i) direct live and dead cell count (Trypan Blue exclusion); (ii) indirectly by mitochondrial activity (resazurin reduction); (iii) indirectly by transcriptional/translational activity (GFP expression). For direct cell count, treated cells were trypsinized with 0.05% trypsin in the CellStripper (Corning)/Ca, Mg-free HBSS (1:1). The treatment media, washings and the trypsinized suspensions were combined, briefly spun at 100 × g and the pellets containing live and dead cells were resuspended in the test media containing 0.2% Trypan Blue. The cells were then counted using a hemacytometer, and the numbers of stained and unstained cells were recorded. To measure the mitochondrial/metabolic activity, adherent treated cells were washed and incubated with 100 μL of the test medium containing 10 mg/L resazurin for 45–60 min. The fluorescence of 50 μL aliquots, along with blanks, was recorded at 540/590 nm. The fluorescence in untreated wells was assigned to 100% proliferation rate and used to normalize the proliferation rates in treated wells. Cell proliferation rates were also evaluated by GFP fluorescence, as a part of the Reporter activity assay, see below.

Reporter Activity Assay

In a typical experiment, immediately after the treatments, the reporter cells were washed and lysed in 60 μL of the Luciferase reporter lysing buffer (Promega). The lysates fluorescence was measured at the 482(9)/512(17) nm wavelength (slit width) setup; this was followed by an addition of the luciferase substrate (Promega), and kinetic luminescence readings in the wells were done in 2-min intervals for 16 min total. All the measurements were done using a Synergy MX (BioTek) plate reader. The GFP fluorescence values were used for both evaluation of relative cell transcriptional activity/proliferation and normalization of the reporter luciferase activities in respective wells (Mossine *et al.*, 2013).

Determination of ATP and ADP

ATP content and the ADP/ATP ratio were determined separately in the test media plus non-adherent cells and in the viable adherent cells using The ApoGlow Adenylate Nucleotide Ratio Assay (Cambrex) following the manufacturer's protocol.

Kinetics of Anaerobic Pyocyanin Reduction

To solutions of 100 μM pyocyanin and 200 μM citrate in Chelex-treated 20 mM HEPES buffer, pH 7.4, were added $FeSO_4$ to 0–5 μM and various chelators or metal salts. The resulting mixtures were transferred to wells of a quartz 96-well plate (Hellma) preloaded with 4 μL of 200 mM glutathione or other reducing agents in quantities calculated for final concentration 2 mM or as indicated. The quartz plate was then rapidly covered with a hydrophobic ink-patterned glass plate MPX96 (Schott Nexterion) such that no air remained in the test wells. The cover was secured by taping and the kinetic runs were initiated at 25 °C by taking O.D. measurements at 500 and 692 nm every 5 min. Kinetic parameters were calculated assuming the zeroth order of the initial and final reaction phases, so that $k_1 = V_1$, $k_3 = V_3$, and Lag time- = abscissa of the intercept of graphs for V_1 and V_{max} (Fig. 5B)

Plotting and Statistical Analysis

Statistical tests and plots were done using SigmaPlot, version 11.0, and **gplots** R package, v.3.0.

RESULTS

Pyocyanin Induces a Dose-Dependent Cell Proliferation Arrest, Extensive ER Vacuolation and Necrotic Death in RTECs

NRK-52E cells stop growing in the complete DMEM/F12 medium after achieving density of about 500 000 cell/cm^2, but readily come out of the quiescent state after splitting. In our experiments, treatments started when the cells were in a log phase, growing from 3.2×10^4 to 1.2×10^5 cells in control wells within 24 h of the experiment (Fig. 1A and B). At pyocyanin concentrations over 30 μM, the cell proliferation rate had significantly slowed down, whereas at >60 μM, the cells appeared progressively hypertrophic and vacuolated (Fig. 1A) until the growing vacuoles fused and burst open. When pyocyanin was withdrawn from NRK-52E after only 12 h of exposure, the cells could recover (>50%) from the PCN doses of up to 400 μM (Fig. 1C), thus indicating a non-programmed cellular fate. Another piece of evidence against a programmed mode of pyocyanin-induced cell death mode in RTECs was obtained when no significant apoptosis of vacuolated cells has been detected within the 24-h treatment period (Supplementary Fig. S1) at any PCN dose. Furthermore, there was a small increase in the cellular ATP content at subtoxic PCN concentrations, whereas the ADP/ATP ratio determined for the dying cells/medium leakage was typical for necrosis (Supplementary Fig. S2).

Next, we examined the vacuoles source. In the stressed NRK-52E cells, the vacuoles failed tests for the lysosomal origin. They were not stained by acidotrophic Acridine Orange and Neutral Red dyes (Fig. 2a and b) or a fluorescent mCherry-tagged lysosome-targeting protein LAMP1 (Supplementary Fig. S3), nor were they labeled by an autophagosome-tracking GFP-LC3 (Fig. 2k and l). Similarly, no vacuolar localization of MitoTracker Green FM (Fig. 2c and d) or mitochondrial membrane-targeting JC-1 (Supplementary Fig. S1) were detected, thus discounting a possibility the vacuoles are of mitochondrial origin. The vacuoles remained unstained by β-1,4-galactosyl transferase

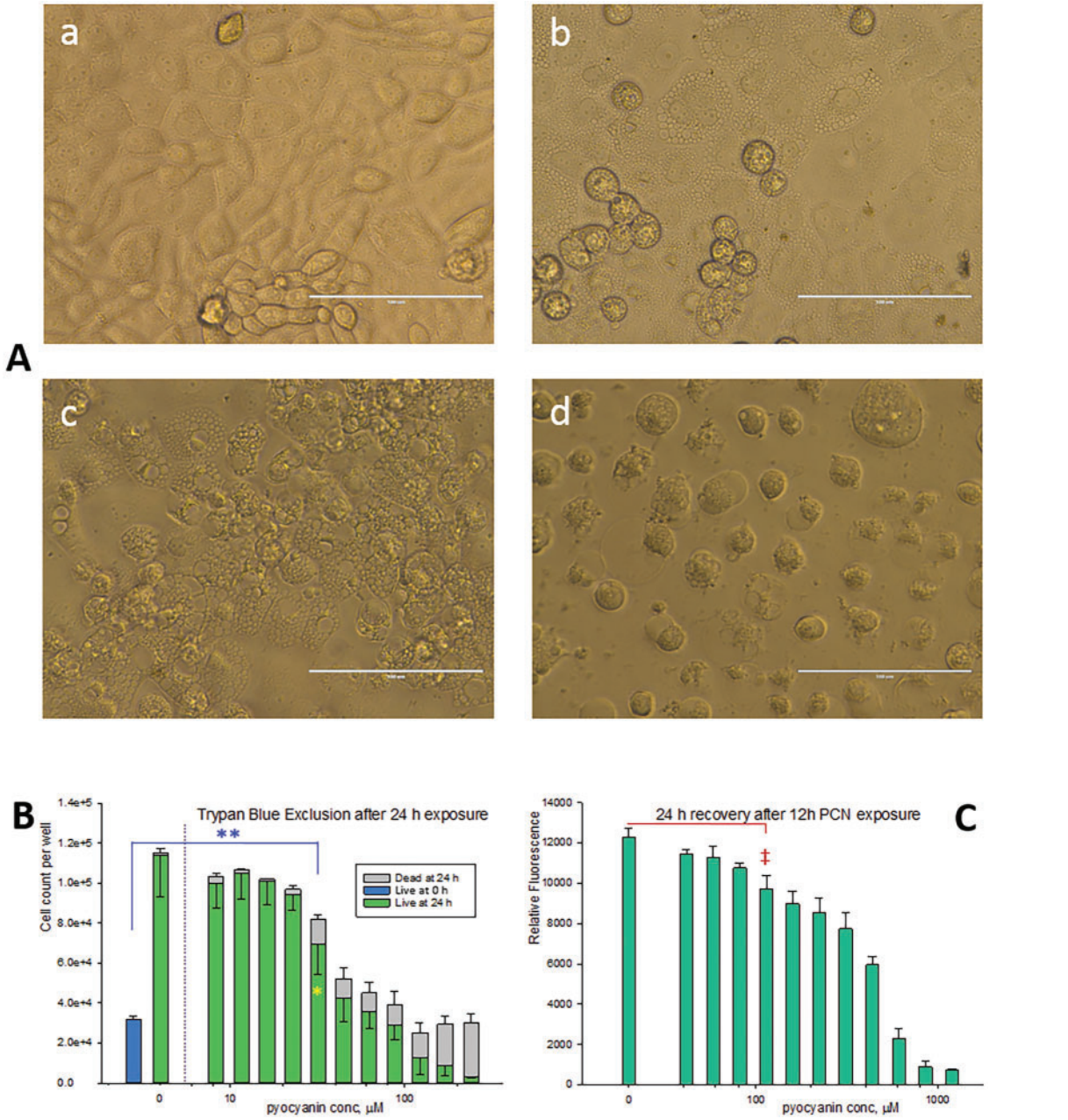

FIG. 1. Pyocyanin is transiently toxic to renal tubular epithelial cells. (A) Phase contrast of NRK-52E cells treated with 87.5 μM pyocyanin (b, c, d) or vehicle (a); after 12 h (b), 18 h (a,c), or 28 h (d). The scale bar: 100 μm. (B) NRK-52E cells were treated with pyocyanin for 24 h, lifted and counted using Trypan Blue exclusion to distinguish between live and dead cells. The blue bar depicts count of live cells at 0 h. Error bars depict SD separately for live and dead cell counts. *Statistics for live cell count: significant, $P < 0.001$, versus control count of live cells at 24 h. **Statistics for live + dead count: significant, $P < 0.001$, versus control of live cells at 0 h. (C) NRK-52E cells were treated with pyocyanin for 12 h, then recovered in fresh medium for 24 h. The relative metabolic activity in wells was determined by the resazurin assay. Error bars are SD. ‡Statistically significant, $P < 0.001$, versus control. All tests done with one-way ANOVA (Holm–Sidak).

tagged with mCherry, a Golgi apparatus-targeting protein in the cells transfected with *p*mCherry-Golgi-7, as well (Fig. 2i and j).

However, the vacuoles were clearly labeled, along with the endoplasmic reticulum (ER), by the ER-targeting calreticulin-mCherry chimera protein in NRK-52E cells transiently transfected with the *p*mCherry-ER-3 vector (Fig. 2g and h). In addition, the cellular distribution of ER-Tracker Green, an ER outer membrane stain, has significantly expanded in the vacuolated cells, with an apparent spread away from the normal subnuclear ER location (Fig. 2e and f). Taken together, these observations lead to a provisional conclusion that the vacuoles are of ER origin and that toxic doses of pyocyanin in NRK-52E cells induce a paraptosis-like (Lee *et al.*, 2016) cell death.

Pyocyanin Induces Maximal Oxidative/Electrophilic Stress Response at Its Subtoxic Doses and Strong Unfolded Protein Response at the Toxic Concentrations

Having identified ER stress as the likely mechanism of PCN *in vitro* toxicity in the RTECs based on the cellular morphology data, we sought an independent line of evidence for the suggested mechanism. Given that vacuolation, the most prominent morphological change, has started developing within 7–8 h of

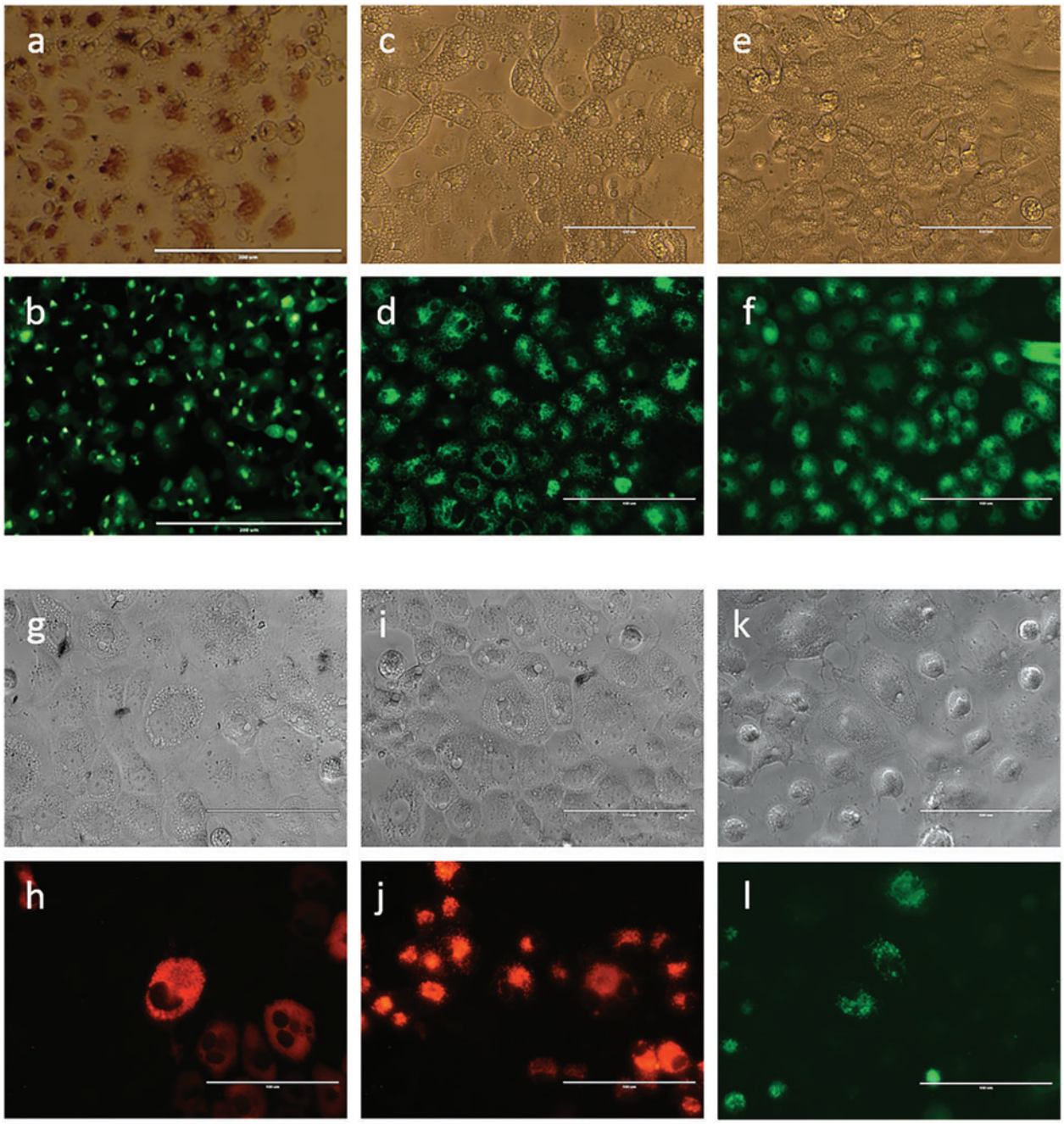

FIG. 2. Identification of the reticular origin for pyocyanin-induced vacuolation in NRK-52E cells. The cells were treated for 20 h with 87.5 μM pyocyanin, then stained with Neutral Red (a), Acridine Orange (b), MitoTracker (c,d), or ER Tracker (e,f). The upper row: phase contrast, the second row: 470/525 nm fluorescence. NRK-52E cells were transiently transfected with fluorescent tracers for endoplasmic reticulum (g,h), Golgi apparatus (i,j), or autophagosomes (k,l) and treated for 10 h with 100 μM pyocyanin. The third row: phase contrast, the lower row: RFP or GFP fluorescence. Scale bar: 200 μm (a,b) or 100 μm (c–l).

the PCN exposure (Supplementary Fig. S4), we considered profiling stress-related transcription factors activation as an adequate alternative mechanistic approach. To perform the task, we have generated several stable NRK-52E lines endowed with reporters for transcriptional activation in response to the cellular stress. Specifically, we employed a novel type of insulated, *piggyBac* transposable reporters (Mossine *et al.*, 2013) which consist of a specific transcription factor response element (TRE), followed by a minimal CMV promoter, a firefly luciferase gene, the Elongation Factor 1 (EF1) promoter for continuous activation of the copepod GFP gene fused with a puromycin resistance sequence through a self-cleavable peptide sequence T2A (Fig. 3A). Such construct allowed for a highly efficient insertion of the reporter sequences into chromatin of transfected NRK-52E cells, as well as their robust expression even in the absence of selecting antibiotics.

To select a timing for the TRE reporter harvesting, we conducted a time-dose-response experiment, whereby dynamics of the cellular response to pyocyanin was evaluated as a transcriptional/translational activity of treated cells through measuring the reporter GFP fluorescence in time series. The resulting diagram (Fig. 3B) indicates that the transcriptional/translational

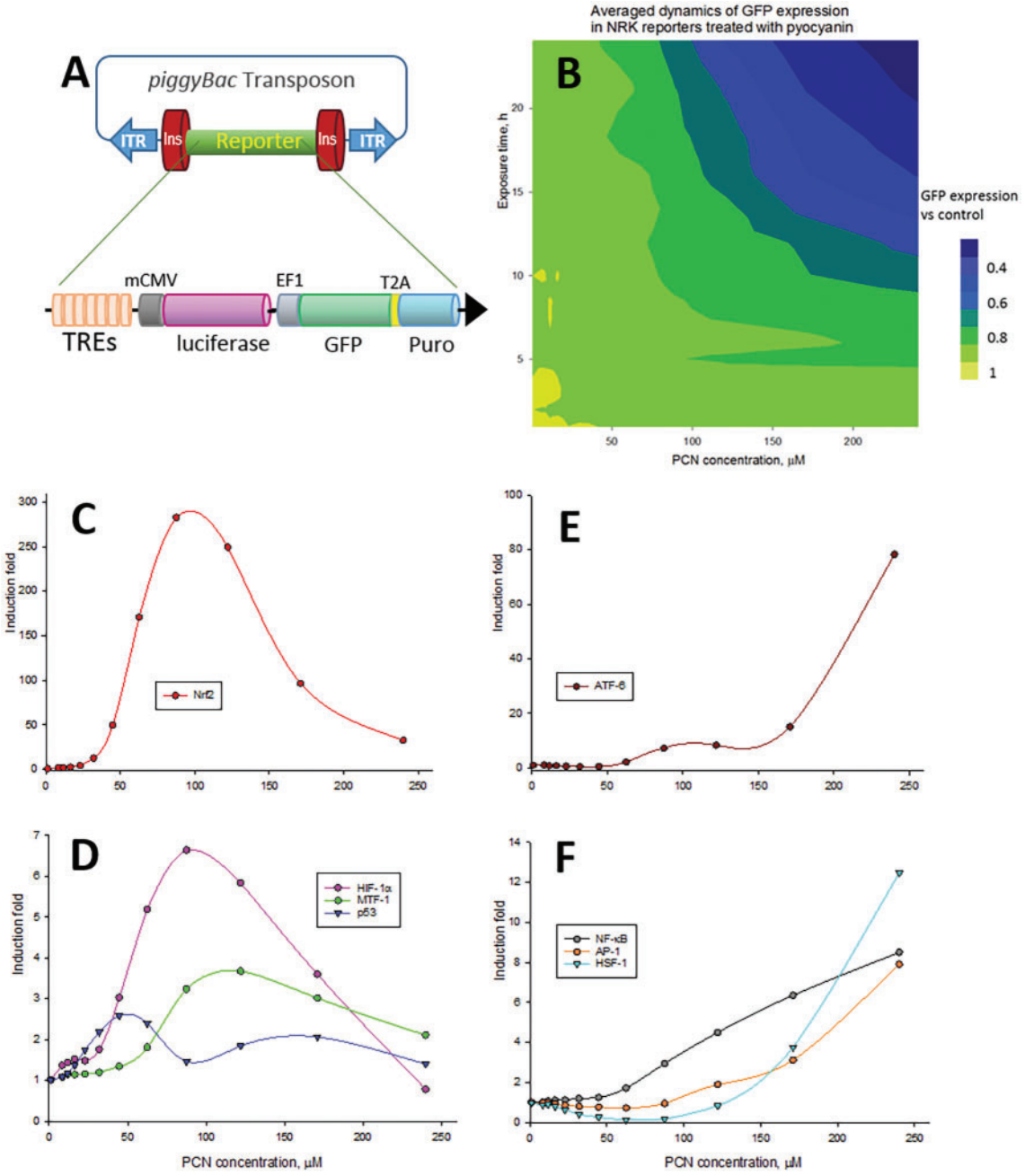

FIG. 3. Profiling pyocyanin-induced stress with insulated reporters of total and specific transcriptional activity. (A) A general scheme of the reporter construct. Four to 8 specific transcription factor (TF) binding sequences (TREs) and mCMV promoter regulate reporter luciferase, whereas EF1 promoter provides for constant production of destabilized GFP and an antibiotic resistance selector. The flanking insulators protect from epigenetic silencing of the reporter, whereas the *piggyBac* transposon ITRs secure accurate and efficient insertion of the reporter into the genomic DNA. (B) An averaged time-dose-response contour plot of relative intracellular GFP fluorescence in 8 NRK.RnnF reporter lines (nn = 01, 03, 05, 09, 12, 13, 15, or 31) treated with pyocyanin. The data arrays used for plotting contained 14 time points × 12 PCN concentrations = 168 fluorescence data points per reporter. These lines report for activities of TFs indicated in the graphs C–F. (C–F) Luciferase induction fold in NRK.RnnF transcriptional activation reporters treated with pyocyanin for 12 h. The luminescence readings are normalized against the respective GFP fluorescence values obtained from the same wells.

activity of PCN treated cells is affected at PCN concentrations above 50–70 μM but does not significantly slow down until about 12 h of the cell exposure to PCN. Accordingly, we carried out 12-h exposures of the reporter cells to PCN before measuring the luciferase activity of the cell lysates that was normalized against the GFP fluorescence of the same lysates. The resulting transcriptional activity profiles are represented in Figure 3C–F. It follows from these data that PCN caused hyperactivation of the transcriptional factors Nrf2 and ATF6 at the subtoxic and toxic PCN doses, respectively. The activation of these TFs is due to a strong oxidative/electrophilic stress response (A/EpR) at subtoxic PCN concentrations (the Nrf2 activity maximum at about 90–100 μM PCN) and a strong unfolded protein response (UPR) at cytotoxic PCN doses (>100 μM). The rest of stress response TF activity patterns have distributed evenly between the aforementioned ones: the HSF-1, NF-κB, and AP-1 show the

increase in their activities towards the cytotoxic PCN exposure, whereas the activation maxima of HIF-1α and MTF-1 were observed at the subtoxic 90–100 μM PCN. Activity of pro-apoptotic p53 was low and reached its maximum at non-toxic 40 μM PCN.

We also tested whether autophagy, a common adaptive response against ER-stress, is activated in the pyocyanin-treated cells. There was a significant increase in an autophagosome marker, LC3-B (also known as LC3-II), in viable NRK-52E cells exposed to PCN for 12 h (Supplementary Fig. S5). The PCN-induced LC3-B production was inhibited by blockers of the autophagosome formation, 3-MA and Wortmannin, whereas the opposite effect was achieved by co-incubation of the cells with the autophagosome degradation blockers, Bafilomycin A and Chloroquine.

Attenuation of the Pyocyanin-Induced Paraptosis Probed by HCA

Upon gaining, through the cellular markers and reporters, an evidence that pyocyanin is likely proteotoxic in RTECs and causes the cellular death through paraptosis-like necrotic pathway, we next sought an additional piece of the mechanistic information through use of a set of specific pathway modulators. A systematic testing of a panel of specific inhibitors of cellular signaling, cellular stress and cellular death pathways (Supplementary Table S2) has been undertaken in order to assess their ability to protect NRK-52E cells from the pyocyanin-induced stress. The protection from paraptosis-like cell injury after 16-h exposure to 80, 120, and 160 μM PCN has been evaluated by 3 criteria: (i) integrity of the cell monolayer; (ii) cell vacuolation, and (iii) the 8-h cell recovery after the PCN/inhibitor removal.

The integrity of cell monolayer was examined microscopically and evaluated by assigning the "stress score", $S = 0$ through 5, with the lowest value assigned to healthy, undisturbed cell monolayer, and the highest S value going to totally distressed cell populations, with no cells properly attached to the well bottom (Supplementary Fig. S6). The extent of the cell vacuolation was also examined microscopically and expressed through the "vacuolation score", $V = 0$ through 3, with the lowest value assigned to wells lacking any evidence of vacuolation, and the highest score signifying vacuoles found in the entire cell population (Supplementary Fig. S6). The resulting High-Content Analysis (HCA) data were visualized as "heat maps", which are shown in Figure 4.

The 8-h cell recovery, evaluated by the mitochondrial activity in the resazurin assay, only loosely correlated with the S score (Fig. 4B) and has shown a relatively high level of recovery even for the cell populations showing the highest stress (over 40% averaged), thus casting a piece of evidence against a programmed character of the cellular death mechanism.

The integration of "stress scores" and the "vacuolation scores" for each tested agent has revealed a direct correlation between the Σ(S) and Σ(V) values (Fig. 4D). These data have identified a group of agents which protected NRK-52E cells from both vacuolation and general stress that were induced by pyocyanin (Supplementary Table S2). One common feature of these agents that apparently correlates with their protective activity is the ability of transition metal chelation. We reasoned that binding transition metal, specifically labile intracellular iron, may be primarily responsible for the cell protection, because non-chelating agents that can inhibit events downstream to iron(II) activity, such as oxidative stress (catalase, SOD, their cell permeable mimic EUK-134, antioxidants BHA, ferulic acid, and resveratrol) or hypoxia (hypoxia mimics Co and Ni) were not protective.

Anaerobic Reduction of Pyocyanin by Glutathione Is Accelerated by Catalytic Iron(II)

A suggestion that PCN cytotoxicity in NRK-52E cells can be better attributed to its iron-dependent proteotoxic potential rather than induction of ROS and oxidative stress has originated from an idea that such proteotoxicity may stem from the ability of PCN to directly oxidize electrophile-sensitive thiol groups in cytosol and ER, such as those sensitive to oxidative/electrophile stress in the KEAP1/Nrf2 complex (Dodson *et al.*, 2015). We reasoned that in the reducing medium of RTECs cytoplasm, PCN could abstract electrons from thiol groups of glutathione and proteins in presence of a redox active metal, such as labile iron. An additional evidence thus was needed for iron mediating the thiol oxidation by PCN. We looked then for a simple chemical model of the PCN – (poly)peptide thiol interaction. The reduced form of PCN, leucopyocyanin, is colorless (Friedheim and Michaelis, 1931) (Fig. 5A), and its formation could be readily monitored spectrophotometrically at 692 nm. When glutathione, Fe^{2+} and citrate were combined with 100 μM PCN at physiologically relevant concentrations and pH in the absence of air, we observed an iron- and GSH concentration-dependent reaction of PCN reduction (Fig. 5B and C and Table 1). Interestingly, the kinetic curves consist of 3 phases: the slowest reaction rate (V_1) is observed in the initial phase that was steady and lasted about 100–200 min in the presence of 2 mM GSH; it is followed by a more rapid second phase of a presumably autocatalytic, iron-independent process, and a slower third phase, which is characterized by a steady rate and its velocity V_3 is also not proportional to the iron concentration (Fig. 5B, Tables 1 and 2). In a set of biologically relevant transition metal ions, such as iron(II), copper(II), zinc(II), manganese(II), or cobalt(II) present at 5 μM concentration, only Fe(II) displayed the ability to catalyze the initial phase of PCN reduction by GSH (Fig. 5C).

We have compared the reducing ability of GSH to other thiols, *N*-acetyl-cysteine and dithiothreitol (DTT), as well as an established intracellular PCN reductant, NADH. There was very rapid, metal-independent reduction of PCN by NADH (data not shown), whereas DTT displayed relatively short, but Fe-dependent initial phase. *N*-Ac-Cys caused a similar, albeit somewhat slower PCN reduction, as compared with GSH (Table 1).

Inhibition of the Pyocyanin—GSH Reaction by Iron Chelators Correlates With the Protection of RTECs From Pyocyanin Proteotoxicity

In order to identify inhibitors of the PCN-GSH reaction from the pool of the agents tested initially in the cell culture, we have selected those compounds that were water-soluble and not cytotoxic on their own at concentrations over 50 μM. In presence of the presumed iron(III/II) chelators, there was a significant decrease in the initial phase rate constants k_1 (Table 2), with an apparent reverse correlation between the k_1 values and the protective potential against the cell vacuolation, Σ(V). On the other hand, we failed to identify any obvious correlations involving other kinetic parameters of the reaction, namely, k_3 and the Lag Time (Table 2).

DISCUSSION

The first conclusion we have gotten in the course of this *in vitro* study is that *P. aeruginosa* virulence factor pyocyanin, at

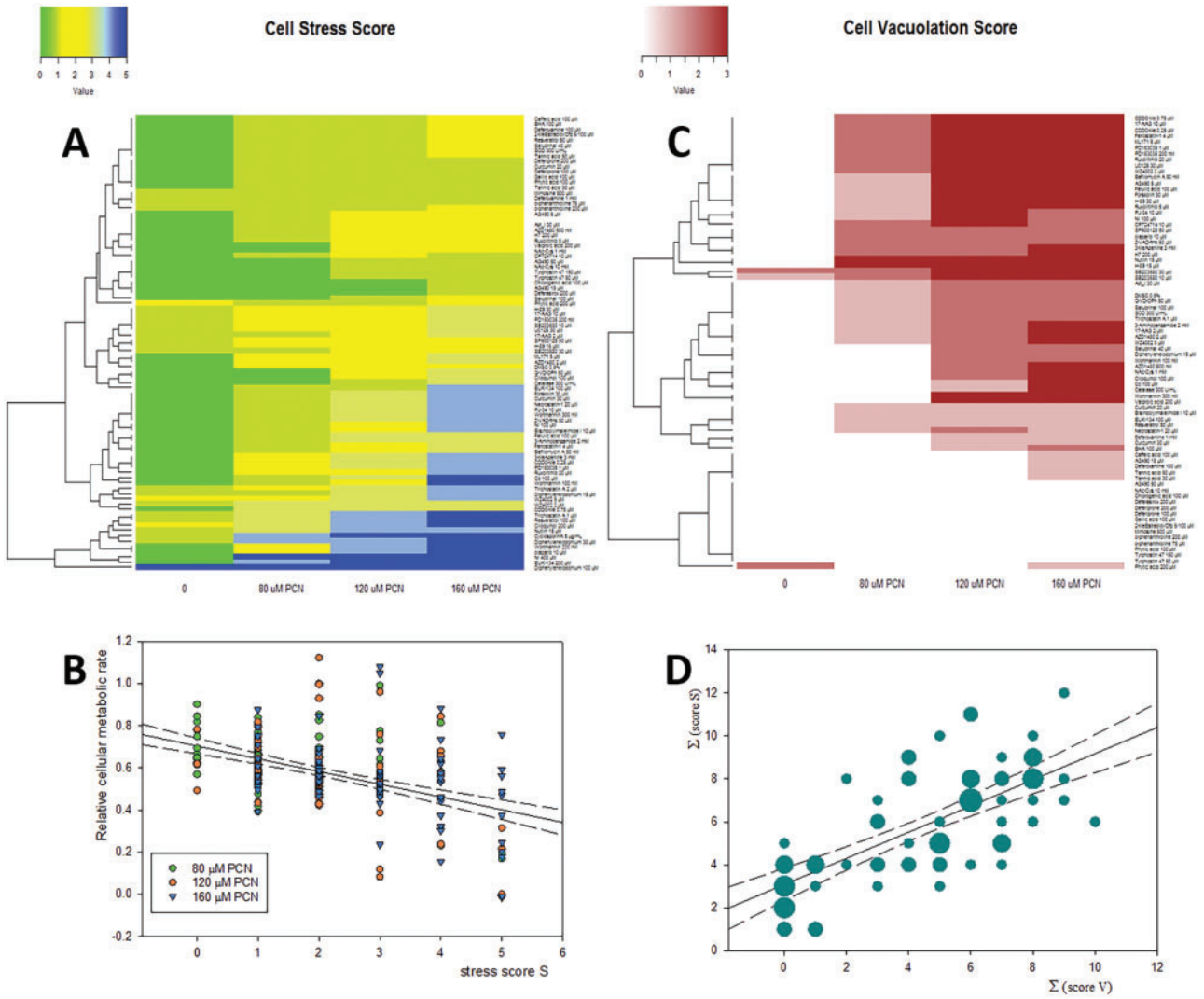

FIG. 4. Protection of NRK-52E cells from pyocyanin-induced stress and vacuolation by a collection of pathway inhibitors listed in Supplementary Table S2. The cells were pretreated with the inhibitors for 1 h, then exposed to pyocyanin at 0, 80, 120, and 160 μM for 16 h. The scoring for stress and vacuolation was done microscopically, the inhibitors/pyocyanin removed, and the cells recovered for next 8 h. (A) A "heat map" summarizing the scores for stress. (B) Correlation between the stress score S and metabolic recovery. Plotted using matching data from (A) and Supplementary Table S2. Shown are 95% confidence intervals for the linear regression, $r^2 = 203$. (C) A "heat map" summarizing scoring for the cellular vacuolation. (D) Correlation between the vacuolation and cellular stress plotted for the matching data from A, C, and Supplementary Table S2. The circles areas are proportional to the number of coinciding experimental points. Shown are 95% confidence intervals for the linear regression, $r^2 = 0.496$.

clinically relevant concentrations (up to 130 μM) (Wilson *et al.*, 1988), can cause cytotoxic effects in renal tubular epithelial cells. The PCN dose-dependent morphological changes included the vacuolation, break of the cell monolayer integrity, rounding up and detachment, progressive disruption of the cellular membrane integrity. The vacuolation of toxin-stressed renal epithelial cells has been well documented in clinical biopsies and autopsies regarding kidney injury or renal failure (Dickenmann *et al.*, 2008; Parai *et al.*, 2012; Perazella, 2003; Zhou *et al.*, 2015), as well as in animal studies (Bendele *et al.*, 1998; Cheng *et al.*, 2012) and *in vitro* experiments (Guyer *et al.*, 2002), where the effect could be reversed by removal of a toxin. In our experiments, the pyocyanin-induced cell vacuolation was accompanied by a drop in the cellular viability, metabolic mitochondrial activity, and decrease in the transcriptional/translational activity. The stressed cells would eventually die or recover, depending whether the PCN exposure had continued or terminated. Hence, results of this study carry a clear relevance to the clinical pathology and toxicology of renal injury.

Next important question we asked: whether the PCN-inflicted cell death is apoptotic or necrotic, attempts to anticipate the immune reaction of the host. Recent publications list a wide range of cell death pathways caused by PCN cytotoxicity, including apoptosis (Forbes *et al.*, 2014; Prince *et al.*, 2008), autophagic death (McFarland *et al.*, 2012) and necrosis (Zhao *et al.*, 2014), along with development of cellular senescence (Muller *et al.*, 2009; Zhao *et al.*, 2014). In our experiments, apoptotic pathway inhibitors failed to protect NRK-52E cells from the PCN-induced cytotoxicity, whereas several molecular markers of apoptosis did not provide any credible evidence in favor of a significant apoptosis. In contrast, microscopical observations of the dying cells offered a picture of necrosis as the main mode of the cellular death. None of the tested inhibitors of programmed necrotic pathways (Galluzzi *et al.*, 2012), including autophagic

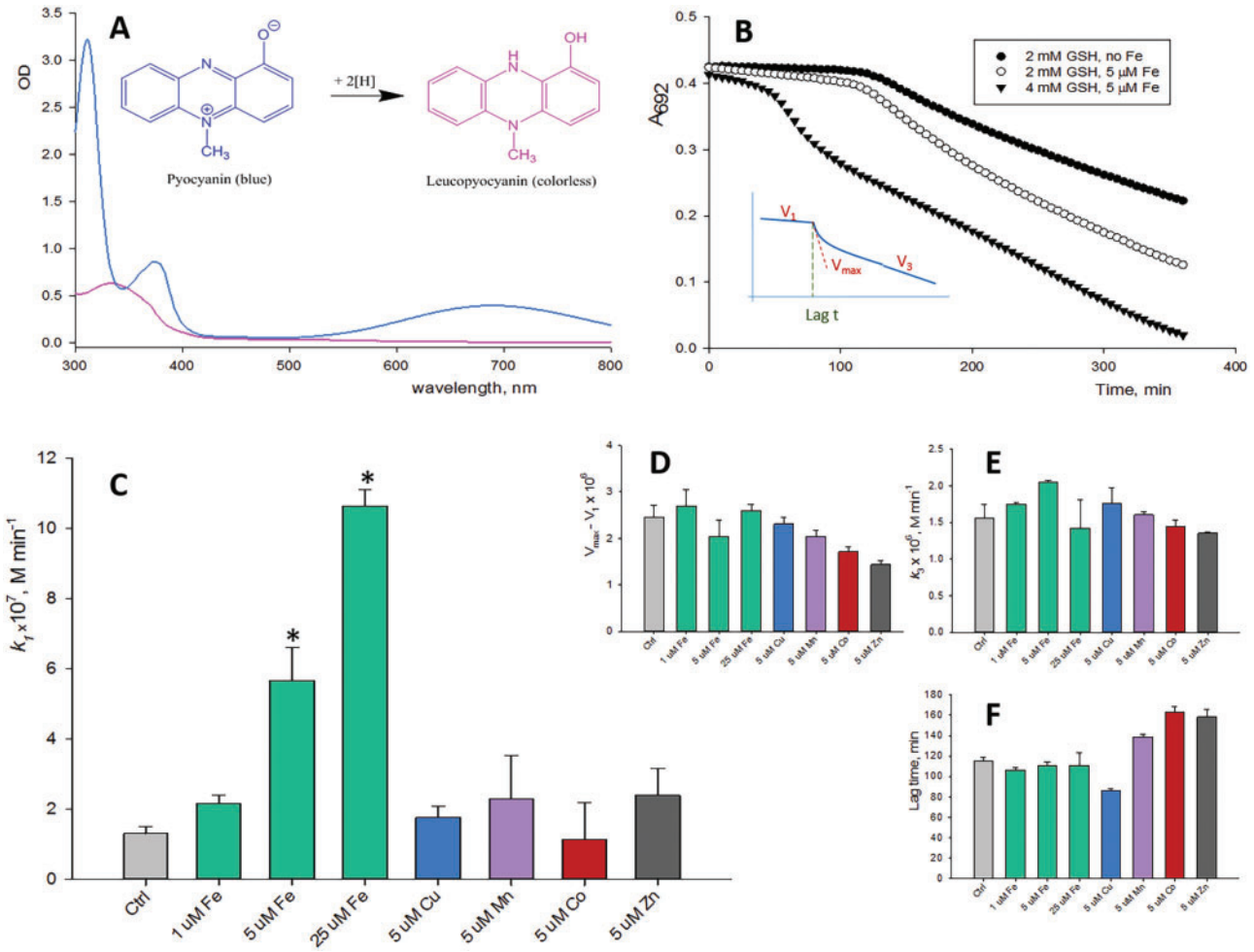

FIG. 5. Anaerobic reduction of pyocyanin by glutathione is catalyzed by iron. (A) Absorption spectra of 100 μM pyocyanin and its reduced form, leucopyocyanin, in 20 mM HEPES, pH 7.5, containing 200 μM citrate, 4 mM glutathione, and the reduction reaction catalyst, 5 μM $FeSO_4$ (pink curve), or the reduction inhibitor, 200 μM DTPA (blue curve). The spectra were taken 12 h after the reaction start at 25 °C. (B) Typical kinetic curves of 100 μM pyocyanin reduction with glutathione. The reaction apparently has 3 phases that can be tentatively described by a set of 4 parameters: the pseudo-zero-order velocities $V_1 = k_1$ and $V_3 = k_3$ for the constant-rate phases, the "lag time", and the V_{max}, as shown in the inset. The relationships between the parameters are unknown. (C–F) Tentative kinetic parameters for the reaction of 100 μM pyocyanin reduction by 2 mM GSH in presence of biologically relevant transition metal ions. Error bars are SD for $n = 3$. *Statistically different (ANOVA, Holm–Sidak test) from the Control, $P < 0.001$.

TABLE 1. "Zero-Order" Kinetic Parameters of Iron-Catalyzed Pyocyanin Reduction

Reductant, inhibitor	Metal ion	$k_1 \times 10^8$, M·min^{-1}	$k_3 \times 10^8$, M·min^{-1}	Lag time, min
GSH 2 mM	–	16 ± 2	202 ± 4	115 ± 4
GSH 2 mM	5 μM Fe	47 ± 5	254 ± 8	123 ± 2
GSH 2 mM DTPA 200 μM	–	0.9 ± 0.8	ND*	>360
GSH 4 mM	–	23 ± 3	216 ± 6	55 ± 1
GSH 4 mM	5 μM Fe	105 ± 7	258 ± 6	25 ± 5
NAcCys 4 mM	–	49 ± 8	54 ± 12	165 ± 5
NAcCys 4 mM	5 μM Fe	53 ± 19	38 ± 39	202 ± 109
NAcCys 4 mM, DTPA 200 μM	–	8.8 ± 1.4	ND	>360
DTT 2 mM	–	8 ± 5	1080 ± 22	26 ± 7
DTT 2 mM	5 μM Fe	16 ± 14	1870 ± 3	<5
DTT 2 mM, DTPA 200 μM	–	8.7 ± 0.6	1160 ± 25	50 ± 5

Setup parameters: 20 mM HEPES, 200 μM citrate, 100 μM pyocyanin, pH 7.5, 25 °C. The values are averages ± SD of $n = 3$ experiments.
*Not determined, due to the Lag time exceeding the overall experiment time.

death, necroptosis, ferroptosis, and parthanatos, could protect the cells from the pyocyanin-induced stress. On the other hand, a withdrawal of PCN from the treatment media as late as after 16-h exposure, when nearly all cells exposed to 160 μM PCN were vacuolated, rounded and nearly detached, did rescue most of these cells, suggesting an absence of any significant death pathway activation at that time. The expansion and fusion of the ER-derived vacuoles suggest a paraptotic type of the cell

TABLE 2. "Zero-Order" Kinetic Parameters of Fe-Catalyzed Pyocyanin Reduction in Presence of the Inhibitors

Inhibitor, concentration	$k_1 \times 10^8$, M·min^{-1}	$k_3 \times 10^8$, M·min^{-1}	Lag time, min	Σ(V); Σ(S)
None; *no iron added*	13 ± 2	157 ± 3	108 ± 3	ND
DTPA 200 μM	1.6 ± 0.3	–*	>360*	ND
Tannic acid 50 μM	8 ± 4	71 ± 4	283 ± 23	1; 4
o-Phenanthroline 100 μM	8 ± 7	335 ± 36	32 ± 7	0; 4
Deferasirox 100 μM	11 ± 4	140 ± 8	104 ± 8	0; 1
Mimosin 100 μM	12 ± 2	160 ± 9	137 ± 3	0; 4
AG490 50 μM	15 ± 8	146 ± 4	118 ± 8	0; 2
Gallic acid 100 μM	18 ± 6	156 ± 5	153 ± 3	0; 3
Deferiprone 100 μM	27 ± 12	156 ± 8	101 ± 17	0; 3
Chlorogenic acid 200 μM	30 ± 25	114 ± 26	142 ± 6	0; 1
Ferrostatin-1 100 μM	33 ± 11	126 ± 8	128 ± 5	8; 6**
Clioquinol 100 μM	34 ± 3	115 ± 14	105 ± 5	5; 5
Caffeic acid 100 μM	38 ± 5	174 ± 3	92 ± 4	1; 4
Ferulic acid 100 μM	39 ± 10	156 ± 7	101 ± 7	7; 7
H-7 100 μM	41 ± 1	221 ± 12	146 ± 10	7; 5
H-89 100 μM	43 ± 16	123 ± 3	88 ± 17	7; 8
3-Aminobenzamide 100 μM	49 ± 11	187 ± 7	103 ± 1	6; 7
DMSO 0.5%	54 ± 12	192 ± 19	92 ± 11	5; 6
None	56 ± 6	231 ± 4	115 ± 2	5; 5

Setup parameters: 20 mM HEPES, 200 μM citrate, 100 μM pyocyanin, 2 mM GSH, 5 μM $FeSO_4$, pH 7.5, 25 °C. The errors are SD for the parameters determined from 3 kinetic curves. The presumed iron chelators are positioned in order of increasing k_1. For the comparison purpose, the selected values Σ(V) and Σ(S), that were determined microscopically in NRK-52E cells co-treated with pyocyanin and the inhibitors, are taken from Supplementary Table S2.

*Lag time is longer than duration of the experiment.

**Values obtained for 4 μM Ferrostatin-1.

death (Cheng *et al.*, 2012). However, the "paraptosis" term assumes a programmed cell death; hence, it would be more appropriate to describe the necrosis of pyocyanin treated NRK-52E cells as a "paraptosis-like" cell death. Currently known mechanisms of the reticular vacuoles formation include: (i) overproduction of unfolded proteins (proteotoxicity) as a result of sulfhydryl homeostasis disruption; (ii) inhibition of the ubiquitin-proteasome pathway leading to accumulation of unfolded proteins in dilated ER; (iii) mitochondrial disfunction (Lee *et al.*, 2016). Because there are no reports that pyocyanin or its structural analogs can impair proteasomal activity and we did not find any evidence for the mitochondrial abnormality in PCN-treated NRK-52E, we turned to a plausible and well documented scenario, according to which PCN can directly disrupt the redox and thiol homeostasis in cells (Muller, 2002; O'Malley *et al.*, 2004; Ray *et al.*, 2015).

A dominant view on the PCN cytotoxicity mechanism considers this redox active compound as a catalyst of the one-electron autoxidation of intracellular substrates such as NAD(P)H and, possibly, glutathione. The ensuing production of ROS in the affected cells brings about oxidative stress (Gloyne *et al.*, 2011; O'Malley *et al.*, 2004; Rada *et al.*, 2008). In this work, we have obtained evidence in favor of a direct proteotoxic, rather than ROS-mediated, mechanism of pyocyanin cytotoxicity. Lines of evidence against a significant contribution of the ROS-mediated oxidative stress included: (i) lack of protection of the PCN-treated cells with small non-chelating antioxidants (phenolics BHA, resveratrol, 1 mM *N*-Ac-Cys, EUK-340) or antioxidant enzymes (catalase, SOD); (ii) lack of a significant p53 activation at cytotoxic PCN concentrations; (iii) intact mitochondrial potential in attached, both normal and vacuolated, cells. The conclusion about pyocyanin proteotoxicity was supported by the strong activation of transcription factors ATF6 and HSF-1, which are sensitive to improperly folded proteins in ER and cytosol and the ER-related paraptotic cell death. The observed hyperactivation of the transcription factor Nrf2, a chief regulator of the oxidative/electrophilic stress response, and a rather moderate activity for the p53 at cytotoxic PCN concentrations is also in concord with an idea that PCN disrupts the intracellular redox homeostasis by targeting thiols directly. Similar conclusions about PCN proteotoxicity have been made recently based on the experiments involving airway epithelial cells (van 't Wout *et al.*, 2015) and *Caernorabdus elegans* (Ray *et al.*, 2015).

On the other hand, we noticed that most of the agents, capable of protecting from the cellular vacuolation and stress, possess a strong iron-binding potential due to presence in their structure one or more metal chelating groups. Such groups include electron-rich oxygen or/and nitrogen atoms associated with aromatic rings, in carboxylates, amines or hydroxylamines, and located at a distance of 3–4 chemical bonds. This arrangement allows for the formation, upon binding of a transition metal ion, of thermodynamically stable 5- or 6-membered chelate rings. For example, among the successful inhibitors of PCN cytotoxicity, we have identified several catechol fragment-bearing compounds (chlorogenic, tannic, and gallic acids, deferiprone, mimosine, Tyrphostins 47 and –AG490) which are expected to selectively bind Fe(III) (Sever and Wilker, 2006). Iron-binding compounds are known for mimicking hypoxia response in cells, as they can deplete cytoplasmic Fe ions and subsequently activate transcription factor HIF-1α (Cho *et al.*, 2013). However, non-chelating activators of HIF-1α cobalt(II) and nickel(II) failed to protect the cytotoxic effects of PCN and, in fact, did synergize with it. This observation discounts the protective potential of HIF-1α and is in agreement with known ability of Co(II) and Ni(II) to replace Fe(II) from the HIF-inhibiting prolyl hydroxylase and other iron proteins, and thus increase concentration of labile cytoplasmic iron.

The idea that iron can mediate oxidation of biologically relevant thiol groups by pyocyanin and that inhibitors of this reaction can protect cells from PCN-induced cytotoxicity was verified by spectrophotometric monitoring of glutathione

oxidation by PCN in anaerobic conditions. The experiment was performed in a 96-well plate and thus allowed for monitoring of a number (typically 36) reactions simultaneously. The technique let molecular oxygen dissolved in the aqueous medium to be present at the beginning of the kinetic run. Air oxygen equilibrates with aqueous solutions at 25 °C within a 200–250 μM range (Millero *et al.*, 2002) and thus could consume up to 1 mM GSH. In most of our experiments, we used 2 mM GSH, an empirically established optimal concentration for good reproducibility of the kinetic data. Because the main purpose of these experiments was to find out whether there is a correlation between the rate of the pyocyanin/glutathione reaction and the severity of PCN-induced cytotoxic effects, we did not attempt to elucidate any chemical mechanisms of this reaction. The unusual shape of the observed kinetic curves would make any mechanistic considerations, without a special investigation, highly speculative. For the comparative purpose, we treated the initial and the terminal parts of the $\mathbf{A_{692}}$ versus **t** plots (Fig. 5B) as reactions of the pseudo-zeroth order, due to their linearity.

Among biologically relevant transition metals introduced into the PCN-GSH system at 5 μM, only Fe induced acceleration of the initial reaction velocity V_1, whereas other, potentially redox active ions such as Cu(II), Co(II), and Mn(II), failed to catalyze the reaction. The observation is somewhat surprising for copper, because Cu is known to catalyze many redox reactions of thiols.

Reduction potential of pyocyanin at pH 7.4 is about −60 mV (Friedheim and Michaelis, 1931) and reduction of PCN at pH > 6 proceeds along a 2-step 2-electron transfer mechanism. This potential allows for PCN reduction by NADH ($E_0' = -320$ mV) and glutathione ($E_0' = -240$ mV) as well as oxidation of reduced PCN by molecular O_2 or Fe(III)-containing species. In extracellular aerobic conditions, GSH and other thiols can deactivate PCN through the oxidative conjugation (Cheluvappa *et al.*, 2008; Muller and Merrett, 2015). We have attributed the protective effect of 10 mM N-Ac-Cys in the cell culture to such reaction. In our anaerobic experiments, however, no intermediate products were detected in the PCN/GSH systems: the visible absorption spectra (400–800 nm) were a simple arithmetic combination of the pyocyanin and leucopyocyanin at any reaction stage, thus excluding accumulation of any colored pyocyanin conjugates or free radicals.

Muller (2011) has suggested earlier that glutathione is incapable of reducing PCN in anaerobic conditions, although his experiments lasted only 5 min. We had the reaction monitored for 6 h, in order to match the timing of the stress response in PCN-treated cells. In our experiments, iron-catalyzed PCN reduction by 2 mM GSH was greatly diminished by the excessive DTPA, one of the strongest conventional Fe(II/III) and other transition metal chelators, so that the "lag time" exceeded 360 min of the kinetic experiment. Nevertheless, the initial rate V_1 value was well detectable, even in absence of any added metal, and had significantly increased upon doubling of GSH concentration or use of a stronger thiol reducing agent DTT (Table 1). Such behavior hints at a possibility of a metal-independent reduction mechanism of PCN by thiols, but more detailed studies are needed to verify this suggestion.

One prospective practical outcome of this work is the finding that compounds capable of strong iron binding can efficiently inhibit cytotoxicity of pyocyanin. A number of iron chelators are approved clinical drugs for both topical and systemic use (Hatcher *et al.*, 2009; Hider, 2014). Pathogenic bacteria require iron for normal growth and employ an arsenal of means, including siderophores and toxins such as PCN, to acquire Fe from the surroundings (Tyrrell and Callaghan, 2016). Hence, restricting Fe availability in the infection sites may help to control the pathogen colonization, whereas our work suggests diminishing of the *P. aeruginosa* virulent factor pyocyanin cytotoxicity to the patient as an additional benefit in this therapeutic approach.

In conclusion, pyocyanin causes reversible proteotoxic stress and induces strong oxidative/electrophilic stress and unfolded protein responses in renal tubular epithelial cells. The pyocyanin cytotoxicity is iron-dependent and can be reduced by iron chelating molecules. Topical or systemic iron chelators deserve an attention as potential therapeutic modalities to help with control of PCN-positive infections.

SUPPLEMENTARY DATA

Supplementary data are available online at http://toxsci.oxfordjournals.org/.

FUNDING

University of Missouri Agriculture Experiment Station Laboratories; the Leda J. Sears Trust Fund; National Institutes of Health (Grant P50AT006273).

REFERENCES

Al-Ani, F. Y., Al-Shibib, A. S., Khammas, K. M., and Taher, R. (1986). Pyocyanin preparation from *Pseudomonas aeruginosa* isolated from heterogeneous clinical materials. *Folia Microbiol.* **31**, 215–219.

Bendele, A., Seely, J., Richey, C., Sennello, G., and Shopp, G. (1998). Renal tubular vacuolation in animals treated with polyethylene-glycol-conjugated proteins. *Toxicol. Sci.* **42**, 152–157.

CDC. Antibiotic resistance threats in the United States, 2013. *U.S. Department of Health and Human Services* [serial online]. Accessed May 3, 2016.

Cheluvappa, R. (2014). Standardized chemical synthesis of *Pseudomonas aeruginosa* pyocyanin. *MethodsX* **1**, 67–73.

Cheluvappa, R., Shimmon, R., Dawson, M., Hilmer, S. N., and Le Couteur, D. G. (2008). Reactions of *Pseudomonas aeruginosa* pyocyanin with reduced glutathione. *Acta Biochim. Pol.* **55**, 571–580.

Cheng, C. H., Shu, K. H., Chang, H. R., and Chou, M. C. (2012). Cyclosporine-induced tubular vacuolization: the role of Bip/Grp78. *Nephron. Exp. Nephrol.* **122**, 1–12.

Cho, E. A., Song, H. K., Lee, S. H., Chung, B. H., Lim, H. M., and Lee, M. K. (2013). Differential in vitro and cellular effects of iron chelators for hypoxia inducible factor hydroxylases. *J. Cell. Biochem.* **114**, 864–873.

Cox, C. D. (1986). Role of pyocyanin in the acquisition of iron from transferrin. *Infect. Immun.* **52**, 263–270.

Czaja, C. A., Scholes, D., Hooton, T. M., and Stamm, W. E. (2007). Population-based epidemiologic analysis of acute pyelonephritis. *Clin. Infect. Dis.* **45**, 273–280.

Das, T., Ibugo Amaye, I., Sehar, S., Manefield, M., Kutty Samuel, K., Tavallaie, R., Panchompoo, J., Aldous, L., Kumar, N., Gooding, J. J., *et al.* (2015). Phenazine virulence factor binding to extracellular DNA is important for *Pseudomonas aeruginosa* biofilm formation. *Sci. Rep.* **5**, 8398.

Dickenmann, M., Oettl, T., and Mihatsch, M. J. (2008). Osmotic nephrosis: acute kidney injury with accumulation of proximal tubular lysosomes due to administration of exogenous solutes. *Am. J. Kidney Dis.* **51**, 491–503.

Dodson, M., Redmann, M., Rajasekaran, N. S., Darley-Usmar, V., and Zhang, J. (2015). KEAP1-NRF2 signalling and autophagy in protection against oxidative and reductive proteotoxicity. *Biochem. J.* **469**, 347–355.

Forbes, A., Davey, A. K., Perkins, A. V., Grant, G. D., McFarland, A. J., McDermott, C. M., and Anoopkumar-Dukie, S. (2014). ERK1/2 activation modulates pyocyanin-induced toxicity in A549 respiratory epithelial cells. *Chem.-Biol. Interact.* **208**, 58–63.

Friedheim, E., and Michaelis, L. (1931). Potentiometric study of pyocyanine. *J. Biol. Chem.* **91**, 355–368.

Galluzzi, L., Vitale, I., Abrams, J. M., Alnemri, E. S., Baehrecke, E. H., Blagosklonny, M. V., Dawson, T. M., Dawson, V. L., El-Deiry, W. S., Fulda, S., *et al.*, (2012). Molecular definitions of cell death subroutines: recommendations of the Nomenclature Committee on Cell Death 2012. *Cell Death Differ.* **19**, 107–120.

Gellatly, S. L., and Hancock, R. E. W. (2013). *Pseudomonas aeruginosa*: new insights into pathogenesis and host defenses. *Pathog. Dis.* **67**, 159–173.

Gloyne, L. S., Grant, G. D., Perkins, A. V., Powell, K. L., McDermott, C. M., Johnson, P. V., Anderson, G. J., Kiefel, M., and Anoopkumar-Dukie, S. (2011). Pyocyanin-induced toxicity in A549 respiratory cells is causally linked to oxidative stress. *Toxicol. In Vitro* **25**, 1353–1358.

Grahl, N., Kern, S. E., Newman, D. K., and Hogan, D. A. (2013). The Yin and Yang of phenazine physiology. In *Microbial Phenazines. Biosynthesis, Agriculture and Health* (S. Chincholkar, and L. Thomashow, Eds.), pp. 43–70. Springer-Verlag, Berlin.

Gupta, P., Gupta, R. K., and Harjai, K. (2013). Quorum sensing signal molecules produced by *Pseudomonas aeruginosa* cause inflammation and escape host factors in murine model of urinary tract infection. *Inflammation* **36**, 1153–1159.

Guyer, D. M., Radulovic, S., Jones, F. E., and Mobley, H. L. T. (2002). Sat, the secreted autotransporter toxin of uropathogenic *Escherichia coli*, is a vacuolating cytotoxin for bladder and kidney epithelial cells. *Infect. Immun.* **70**, 4539–4546.

Hatcher, H. C., Singh, R. N., Torti, F. M., and Torti, S. V. (2009). Synthetic and natural iron chelators: therapeutic potential and clinical use. *Future Med. Chem.* **1**, 1643–1670.

Heussner, A. H., and Dietrich, D. R. (2013). Comparison of two renal cell lines (NRK-52E and LLC-PK1) as late stage apoptosis models. *Open J. Apoptosis* **2**, 25–30.

Hider, R. (2014). Recent developments centered on orally active iron chelators. *Thalassemia Rep.* **4**, 2261.

Kanthakumar, K., Cundell, D. R., Johnson, M., Wills, P. J., Taylor, G. W., Cole, P. J., and Wilson, R. (1994). Effect of salmeterol on human nasal, epithelial cell ciliary beating: inhibition of the ciliotoxin, pyocyanin. *Br. J. Pharmacol.* **112**, 493–498.

Lagun, L. V., Atanasova, Y. V., and Tapal'skii, D. V. (2013). Formation of microbial biofilms in causative agents of acute and chronic pyelonephritis. *Russ. J. Microbiol.* **3**, 18–23.

Lee, D., Kim, I. Y., Saha, S., and Choi, K. S. (2016). Paraptosis in the anti-cancer arsenal of natural products. *Pharmacol. Ther.* **162**, 120–133.

Lee, I. H., Cao, L., Mostoslavsky, R., Lombard, D. B., Liu, J., Bruns, N. E., Tsokos, M., Alt, F. W., and Finkel, T. (2008). A role for the NAD-dependent deacetylase Sirt1 in the regulation of autophagy. *Proc. Natl. Acad. Sci. U.S.A.* **105**, 3374–3379.

McFarland, A. J., Anoopkumar-Dukie, S., Perkins, A. V., Davey, A. K., and Grant, G. D. (2012). Inhibition of autophagy by 3-methyladenine protects 1321N1 astrocytoma cells against pyocyanin- and 1-hydroxyphenazine-induced toxicity. *Arch. Toxicol.* **86**, 275–284.

Miceli, M. H., Diaz, J. A., and Lee, S. A. (2011). Emerging opportunistic yeast infections. *Lancet Infect. Dis.* **11**, 142–151.

Millero, F. J., Huang, F., and Laferiere, A. L. (2002). The solubility of oxygen in the major sea salts and their mixtures at 25 °C. *Geochim. Cosmochim. Acta* **66**, 2349–2359.

Mossine, V. V., Waters, J. K., Hannink, M., and Mawhinney, T. P. (2013). *piggyBac* Transposon plus insulators overcome epigenetic silencing to provide for stable signaling pathway reporter cell lines. *PLoS One* **8**, e85494.

Muller, M. (2002). Pyocyanin induces oxidative stress in human endothelial cells and modulates the glutathione redox cycle. *Free Radic. Biol. Med.* **33**, 1527–1533.

Muller, M. (2006). Premature cellular senescence induced by pyocyanin, a redox-active *Pseudomonas aeruginosa* toxin. *Free Radic. Biol. Med.* **41**, 1670–1677.

Muller, M. (2011). Glutathione modulates the toxicity of, but is not a biologically relevant reductant for, the *Pseudomonas aeruginosa* redox toxin pyocyanin. *Free Radic. Biol. Med.* **50**, 971–977.

Muller, M., Li, Z., and Maitz, P. K. M. (2009). *Pseudomonas* pyocyanin inhibits wound repair by inducing premature cellular senescence: role for p38 mitogen-activated protein kinase. *Burns* **35**, 500–508.

Muller, M., and Merrett, N. D. (2015). Mechanism for glutathione-mediated protection against the *Pseudomonas aeruginosa* redox toxin, pyocyanin. *Chem.-Biol. Interact.* **232**, 30–37.

O'Malley, Y. Q., Reszka, K. J., Rasmussen, G. T., Abdalla, M. Y., Denning, G. M., and Britigan, B. E. (2003). The *Pseudomonas* secretory product pyocyanin inhibits catalase activity in human lung epithelial cells. *Am. J. Physiol.* **285**, L1077–L1086.

O'Malley, Y. Q., Reszka, K. J., Spitz, D. R., Denning, G. M., and Britigan, B. E. (2004). *Pseudomonas aeruginosa* pyocyanin directly oxidizes glutathione and decreases its levels in airway epithelial cells. *Am. J. Physiol.* **287**, L94–L103.

Önal, S., Aridogan, B. C., Gönen, I., Tas, T., and Kaya, S. (2015). Virulence factors of *Pseudomonas aeruginosa* strains isolated from clinical samples and role of quorum sensing signal molecules in the pathogenesis of the disease. *Acta Med. Mediterr.* **31**, 851–856.

Orenstein, R., and Wong, E. S. (1999). Urinary tract infections in adults. *Am. Fam. Physician* **59**, 1225–1237.

Parai, J. L., Kodikara, S., Milroy, C. M., and Pollanen, M. S. (2012). Alcoholism and the Armanni-Ebstein lesion. *Forensic Sci. Med. Pathol.* **8**, 19–22.

Perazella, M. A. (2003). Drug-induced renal failure: update on new medications and unique mechanisms of nephrotoxicity. *Am. J. Med. Sci.* **325**, 349–362.

Prince, L. R., Bianchi, S. M., Vaughan, K. M., Bewley, M. A., Marriott, H. M., Walmsley, S. R., Taylor, G. W., Buttle, D. J., Sabroe, I., Dockrell, D. H., and Whyte, M. K. (2008). Subversion of a lysosomal pathway regulating neutrophil apoptosis by a major bacterial toxin, pyocyanin. *J. Immunol.* **180**, 3502–3511.

Rada, B., Gardina, P., Myers, T. G., and Leto, T. L. (2011). Reactive oxygen species mediate inflammatory cytokine release and EGFR-dependent mucin secretion in airway epithelial cells exposed to *Pseudomonas* pyocyanin. *Mucosal. Immunol.* **4**, 158–171.

Rada, B., Lekstrom, K., Damian, S., Dupuy, C., and Leto, T. L. (2008). The *Pseudomonas* toxin pyocyanin inhibits the dual oxidase-based antimicrobial system as it imposes oxidative stress on airway epithelial cells. *J. Immunol.* **181**, 4883–4893.

Rada, B., and Leto, T. L. (2009). Redox warfare between airway epithelial cells and Pseudomonas: dual oxidase versus pyocyanin. *Immunol. Res*. **43**, 198–209.

Ray, A., Rentas, C., Caldwell, G. A., and Caldwell, K. A. (2015). Phenazine derivatives cause proteotoxicity and stress in *C. elegans*. *Neurosci. Lett*. **584**, 23–27.

Schwarzer, C., Fischer, H., Kim, E. J., Barber, K. J., Mills, A. D., Kurth, M. J., Gruenert, D. C., Suh, J. H., Machen, T. E., and Illek, B. (2008). Oxidative stress caused by pyocyanin impairs CFTR Cl- transport in human bronchial epithelial cells. *Free Radical Biol. Med*. **45**, 1653–1662.

Senft, A. P., Dalton, T. P., and Shertzer, H. G. (2000). Determining glutathione and glutathione disulfide using the fluorescence probe o-phthalaldehyde. *Anal. Biochem*. **280**, 80–86.

Sever, M. J., and Wilker, J. J. (2006). Absorption spectroscopy and binding constants for first-row transition metal complexes of a DOPA-containing peptide. *Dalton Trans*. 813–822.

Silva, L. V., Branquinha, M. H., Galdino, A. C. M., Nunes, A. P. F., dos Santos, K. R. N., Moreira, B. M., Cacci, L. C., Sodré, C. L., Ziccardi, M., and Santos, A. L. S. (2014). Virulence attributes in Brazilian clinical isolates of *Pseudomonas aeruginosa*. *Int. J. Med. Microbiol*. **304**, 990–1000.

Strateva, T., and Mitov, I. (2011). Contribution of an arsenal of virulence factors to pathogenesis of *Pseudomonas aeruginosa* infections. *Ann. Microbiol*. **61**, 717–732.

Tyrrell, J., and Callaghan, M. (2016). Iron acquisition in the cystic fibrosis lung and potential for novel therapeutic strategies. *Microbiology* **162**, 191–205.

van 't Wout, E. F. A., van Schadewijk, A., van Boxtel, R., Dalton, L. E., Clarke, H. J., Tommassen, J., Marciniak, S. J., and Hiemstra, P. S. (2015). Virulence factors of *Pseudomonas aeruginosa* induce both the unfolded protein and integrated stress responses in airway epithelial cells. *PLoS Pathog*. **11**, e1004946.

Weinstein, R. A., Molton, J. S., Tambyah, P. A., Ang, B. S. P., Ling, M. L., and Fisher, D. A. (2013). The global spread of healthcare-associated multidrug-resistant bacteria: a perspective from Asia. *Clin. Infect. Dis*. **56**, 1310–1318.

Wilson, R., Sykes, D. A., Watson, D., Rutman, A., Taylor, G. W., and Cole, P. J. (1988). Measurement of *Pseudomonas aeruginosa* phenazine pigments in sputum and assessment of their contribution to sputum sol toxicity for respiratory epithelium. *Infect. Immun*. **56**, 2515–2517.

Zhao, J., Wu, Y., Alfred, A. T., Wei, P., and Yang, S. (2014). Anticancer effects of pyocyanin on HepG2 human hepatoma cells. *Lett. Appl. Microbiol*. **58**, 541–548.

Zhou, C., Moore, L., Yool, A., Jaunzems, A., and Byard, R. W. (2015). Renal tubular epithelial vacuoles—a marker for both hyperlipidemia and ketoacidosis at autopsy. *J. Forensic Sci*. **60**, 638–641.